

DETERMINATION OF THE PSEUDOPOTENTIAL FOURIER COMPONENTS

ON THE BASIS OF INTERBAND TRANSITIONS IN THE OPTICAL RANGE

A. I. GOLOVASHKIN, A. I. KOPELIOVICH and G. P. MOTULEVICH

P. N. Lebedev Physics Institute, Academy of Sciences, USSR

Submitted June 2, 1967

Zh. Eksp. Teor. Fiz. 53, 2053-2062 (December, 1967)

Interband transition in non-transition metals, connected with Bragg reflections of electrons, are considered. An expression is obtained for the interband conductivity $\tilde{\sigma}$. It is shown that the presence of Bragg reflections leads to the appearance of maxima in the dependence of the interband conductivity on the light frequency. The location of these maxima makes it possible to determine the pseudopotential Fourier coefficients. The theory is compared with the experimental results obtained for aluminum and indium. Satisfactory agreement is observed between theory and experiment.

1. At the present time, the concept of the pseudopotential, introduced by Harrison^[1] and developed by a number of authors, is frequently used in solid state physics. The theory of the pseudopotential operates with the Fourier components of the pseudopotential V_g . These Fourier components have recently been determined from experiment, principally from the de Haas-van Alphen effect.^[2,3] However, a more direct and simpler method is the determination of V_g from optical measurements. The connection of the values of V_g with the conductivity at optical frequencies has been used by us in^[4]. In the present research, a detailed consideration is given to the determination of the Fourier components of the pseudopotential from the results of optical measurements in the visible and near infrared portions of the spectrum. It will be shown that the structure of the absorption band in this region of the spectrum, determined by interband transitions, is connected with the presence of Bragg reflections.

In semiconductors, the structure of the absorption band is connected with the presence of critical points. Initially, the role of critical points was studied by van Hove and Phillips^[5] for lattice vibrations. Later, similar ideas were applied by Phillips, Brust, et al.^[6] to the optical properties of solids. The critical points are determined by the condition $\nabla_p E_{ij}(p) = 0$. Here $E_{ij}(p) = E_i(p) - E_j(p)$, where $E_i(p)$ is the energy of the electrons in band i for momentum p . Usually the critical points are points of high symmetry in momentum space. Near the critical points, the constant energy surfaces are approximately parallel, thanks to which a peak is obtained in the combined interband density of states $dY/d\omega$. Here dY is the number of states in the frequency range of the interband transitions from ω to $\omega + d\omega$.

In polyvalent metals, the presence of Bragg planes leads to the result that finite portions of these planes possess singular features. For this reason, a large number of electrons will take part in the corresponding interband transitions. This number is larger than in transitions which are connected with the presence of isolated critical points. This leads to the result that the structure of the absorption band in the region of the spectrum of ω close to $2|V_g|$ is essentially determined by the presence of these planes.

We shall assume that the inequality

$$|V_g| \ll E_F^0, \tag{1}$$

is valid, where E_F^0 is the Fermi energy corresponding to free electrons. This means that one can use the approximation of weakly coupled electrons. Taking also into account the additivity of the conductivity σ associated with interband transitions, we can consider the contribution of each plane to this quantity independently.

2. We consider the intersection of the sphere of free electrons by a single Bragg plane (see Figs. 1 and 2). The wave functions of the electrons near the Bragg plane are satisfactorily described by the sum of two plane waves:

$$\exp\left(i\frac{\mathbf{p}}{\hbar}\mathbf{r}\right), \quad \exp\left(i\frac{\mathbf{p}-2\mathbf{p}_g}{\hbar}\mathbf{r}\right).$$

here $\mathbf{p}_g = \hbar\mathbf{g}/2$, where \mathbf{g} is the reciprocal lattice vector for the Bragg plane considered, \mathbf{p} is the momentum of the electron. Here the wave functions of the electron in the lower and upper bands, normalized to unit volume, are equal to

$$\psi_1 = a_{11}\exp\left(i\frac{\mathbf{p}}{\hbar}\mathbf{r}\right) + a_{12}\exp\left[i\frac{\mathbf{p}-2\mathbf{p}_g}{\hbar}\mathbf{r}\right] \tag{2}$$

$$\psi_2 = a_{21}\exp\left(i\frac{\mathbf{p}}{\hbar}\mathbf{r}\right) + a_{22}\exp\left[i\frac{\mathbf{p}-2\mathbf{p}_g}{\hbar}\mathbf{r}\right];$$

$$a_{11} = 2^{-1/2}(1+x^2-x\sqrt{1+x^2})^{-1/2}, \quad a_{12} = a_{11}(x-\sqrt{1+x^2}), \tag{3}$$

$$a_{21} = 2^{-1/2}(1+x^2+x\sqrt{1+x^2})^{-1/2}, \quad a_{22} = a_{21}(x+\sqrt{1+x^2}); \tag{4}$$

$$x = p_g(p_g - p_\perp) / m|V_g|.$$

Here m is the mass of the free electron, p_\perp the projection of the vector \mathbf{p} on the normal to the Bragg plane.

The difference in energy between the upper and lower bands for vertical transitions in the presented band scheme is equal to

$$\Delta E = 2|V_g|\sqrt{1+x^2}. \tag{5}$$

It is convenient to introduce the notation

$$\hbar\omega_g = 2|V_g|. \tag{6}$$

For the calculation of the interband conductivity associated with the Bragg plane g , we use the following relation (for simplicity, we limit ourselves to a

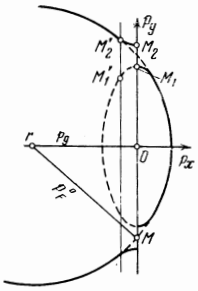


FIG. 1. Intersection of the sphere of free electrons with a Bragg plane. The Bragg plane coincides with the plane $p_y p_z$. The plane $M_1' M_2'$ is parallel to the Bragg plane.

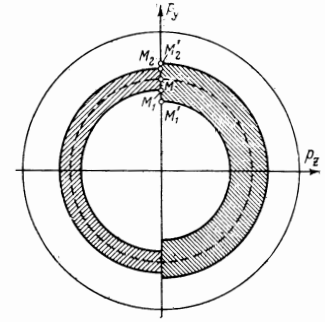


FIG. 2. Ring between the circles obtained from intersection of the Fermi surface with the Bragg plane ($M_1 M_2$) and the plane parallel to it ($M_1' M_2'$).

cubic crystal):¹⁾

$$\tilde{\sigma}_\alpha = \frac{w_g \hbar \omega}{e^2} = \frac{1}{8\pi^2} \frac{e^2}{m^2 c^2 \hbar^2} \frac{\omega}{e^2} \int |\langle \psi_1 | \nabla A | \psi_2 \rangle|^2 \delta(\Delta E - \hbar \omega) d^3 p, \quad (7)$$

$$A(t) = \frac{1}{2} (A e^{-i\omega t} + A^* e^{i\omega t}). \quad (8)$$

Here w_g is the transition probability with energy difference ΔE under the action of light of frequency ω ; ϵ is the electric field of the light wave; $A(t)$ is the vector potential of the electromagnetic field. The bar denotes averaging over time. Here the Hamiltonian of interaction of the electrons with the electromagnetic field is used:

$$\mathcal{H}_i(t) = i(\hbar e / mc) \nabla A(t).$$

We have neglected terms proportional to A^2 .

Equation (7) does not take into account relaxation processes. In this case, the following relations hold:

$$\Delta E = \hbar \omega = \hbar \omega_g \sqrt{1 + x^2} \quad (9)$$

and

$$\tilde{\sigma}_g = \frac{2\pi}{\hbar} \frac{1}{4} \frac{e^2 \hbar^2}{m^2 c^2} |\langle \psi_1 | \nabla A | \psi_2 \rangle|^2 \frac{\omega}{e^2} \frac{dY}{d\omega}, \quad (10)$$

where $dY/d\omega$ is the combined interband density of states.

It follows from (2) and (3), if we neglect the dependence of A on the coordinates, that

$$|\langle \psi_1 | \nabla A | \psi_2 \rangle|^2 = \frac{1}{\hbar^2} \frac{1}{1 + x^2} (A p_g)^2. \quad (11)$$

For calculation of the combined interband density of states, we turn to Fig. 1. We consider the plane $M_1' M_2'$ parallel to the Bragg plane. For it, $p_\perp = \text{const}$, and, according to (4) and (5), $x = \text{const}$ and $\Delta E = \text{const}$. We need to determine a region on this plane for which the lower state is occupied and the upper free. Such a region is the ring contained between the two circles which result from the intersection of the Fermi surface with the plane under consideration. In Figs. 1 and 2, this ring is $M_1' M_2'$, on the Bragg plane itself, this ring is $M_1 M_2$. For it, $x = 0$, and the difference in the energies is minimal and is equal to

$$\Delta E_g = 2|V_g| = \hbar \omega_g. \quad (12)$$

The combined interband density of states is equal to

$$\frac{dY}{d\omega} = 2S \frac{dp_\perp}{(2\pi\hbar)^3}. \quad (13)$$

Here S is the area of the ring $M_1' M_2'$ in momentum space. It is not difficult to find that

$$S = 4\pi m |V_g| \sqrt{1 + x^2}. \quad (14)$$

Taking (4) and (9) into account, we obtain

$$\begin{aligned} \frac{dY}{d\omega} &= -\frac{m^2}{4\pi^2 \hbar p_g} \frac{\omega^2}{\omega \sqrt{\omega^2 - \omega_g^2}} \quad \text{for } \omega > \omega_g, \\ \frac{dY}{d\omega} &= 0 \quad \text{for } \omega < \omega_g. \end{aligned} \quad (15)$$

A similar relation was obtained by Harrison^[7] for the combined interband density of states. His expression differs from (15) inasmuch as he used the expansion in the small parameter x and did not take into account the change in the area of the ring S with change in x .

It follows from (10), (11), and (15) that

$$\tilde{\sigma}_g = \frac{e^2 p_g \cos^2 \theta_g}{4\pi \hbar^2} \frac{\omega_g^2}{\omega \sqrt{\omega^2 - \omega_g^2}}. \quad (16)$$

Here θ_g is the angle between ϵ and p_g . For polycrystals, one has the mean value $\cos^2 \theta_g = 1/3$. Considering all the physically equivalent Bragg planes $\{g\}$, we obtain

$$\tilde{\sigma}_{(g)} = \frac{e^2}{12\pi \hbar^2} \frac{n_g p_g}{\omega \sqrt{\omega^2 - \omega_g^2}}. \quad (17)$$

Here n_g is the number of physically equivalent planes g . This formula is valid also for cubic single crystals.

The total conductivity is

$$\sigma = \sum \tilde{\sigma}_{(g)}. \quad (18)$$

Summation is carried out over all planes that make a contribution to the interband conductivity. The curly brackets for the index g will be omitted below. For $\omega \gg \omega_g$, we have

$$\tilde{\sigma}_g = \frac{e^2}{12\pi \hbar^2} n_g p_g \left(\frac{\omega_g}{\omega}\right)^2. \quad (19)$$

3. It follows from (17) that the interband conductivity is suddenly "turned on" at $\omega = \omega_g$ and goes to infinity at this point. Both these circumstances are connected, first of all, with the fact that an approximation is used in which the wave function of the electron is equal to the sum of only two plane waves. This means that each time the action of only a single Bragg plane is considered. Account of the simultaneous action of several planes leads to a finite value of the maximum. It can be expected that the width of this will be of the order of $|V_g|/E_F$. Second, we have neglected relaxation processes, which also lead to a finite value of the maximum and to an increase in its width.

¹⁾In Eq. (7), there has been omitted from the integral a factor equal to the difference in the probabilities of filling the initial and final states, inasmuch as it is equal to unity for our case ($\hbar \omega \gg kT$).

Account of relaxation processes is apparently more important than account of the simultaneous action of several planes. An experiment carried out by us for indium^[4] and lead^[8] shows that $\Delta\omega/\omega_g \approx 0.2$ even for helium temperatures ($\Delta\omega$ is the half-width of the maximum). Upon increase in the temperature, this quantity increases.

Short lifetimes of the excited states can be connected with the strong inter-electronic interaction. This interaction is much greater than the corresponding interaction for electrons situated on the Fermi surface, inasmuch as the energy of the ground and excited states differ from E_F by an amount that is much larger than kT . Moreover, since the constant energy bands are parallel, the phase volume in which the electron can be scattered is large if the energy conservation is satisfied.

Another reason for a decrease in the lifetime of the excited states is the interaction of the electrons with the phonons. It is well known that the interaction of electrons near a Bragg plane with the static potential of the lattice, by virtue of the corresponding phase relations, is so great that these electrons cannot propagate through the crystal. Therefore, it can be expected that the interaction of these electrons with phonons will be much greater than the interaction of the electrons situated far from the Bragg plane.

Correct account of relaxation processes demands the setting up and solution of the kinetic equation for the case under consideration. So far as we know, such a program has not been carried out to date. However, in first approximation, one can take into account the relaxation processes with the help of replacement of the δ function in Eq. (7) by the Lorentz function φ . We use the relation

$$\delta(\xi) = \lim_{\gamma \rightarrow 0} \varphi(\xi) \quad \text{as } \gamma \rightarrow 0,$$

where

$$\varphi(\xi) = \frac{\gamma}{\pi} \frac{1}{\xi^2 + \gamma^2}. \quad (20)$$

One can assume that, in first approximation, γ does not depend on the frequency²⁾.

In what follows, it will be convenient to use the dimensionless quantities

$$\omega' = \omega / \omega_g, \quad \gamma' = \gamma / \hbar\omega_g. \quad (21)$$

In these variables,

$$\xi / \hbar\omega_g = \sqrt{1 + x^2} - \omega'. \quad (22)$$

Using (7), (20), and (22), we get

$$\tilde{\sigma}_g = \frac{1}{12} \frac{e^2}{\pi^2 \hbar^2} n_g p_g I, \quad (23)$$

$$I = \frac{\gamma'}{\omega'} \int_0^{\infty} \frac{dx}{\sqrt{1+x^2}[(\sqrt{1+x^2}-\omega')^2 + \gamma'^2]}. \quad (24)$$

Calculation of the integral carried out above gives no difficulties, inasmuch as the expression for the inhomogeneous integral can be obtained from tables.^[9] For a specific value of γ' , the integral I is a function of ω' . We shall consider the function $I(\omega')$, assuming γ' to be a parameter. The calculation shows that $I(\omega')$

²⁾ Similar results are obtained if we use other appropriate expressions for $\varphi(\xi)$.

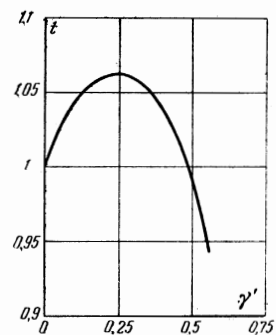


FIG. 3. Dependence of the quantity $t = \omega_{\max}/\omega_g$ on γ' .

has a finite maximum in the region $\omega' \approx 1$. The shift of the position of this maximum is determined by the coefficient $t = \omega_{\max}/\omega_g$, the value of which is shown in Fig. 3 as a function of γ' . Using the graph of this drawing and the experimental value of the frequency ω_{\max} , which corresponds to the maximum of the conductivity, we can determine the pseudopotential Fourier component V_g from the formula

$$2|V_g| = \hbar\omega_g = \hbar\omega_{\max} / t. \quad (25)$$

As is seen in Fig. 3, the shift of the maximum is small. The greatest shift amounts to $\sim 6\%$. Therefore, the coefficient t can be assumed to be equal to unity to within 5–6%.

Figure 4 shows the dependence of the maximum value of the integral I for different values of the parameter γ' . It follows from Eq. (23) and Fig. 4 that the value of the maximum $\tilde{\sigma}_{\max}$ depends only on the relative value of $\gamma' = \gamma/\hbar\omega_g$ and on the product $n_g p_g$.

Figure 5 gives the dependence of the value of I on ω' for different values of the parameter γ' . It is seen that the curves are asymmetric. It can be expected that these curves will describe the experimental results sufficiently well in the region of $\omega' \ll 1 - \gamma'$, these formulas are not valid, inasmuch as the replacement of the δ function by the Lorentzian function at these frequencies is too rough an approximation. In the region $\omega' - 1 \gg \gamma'$, the asymptotic dependence (19) is obtained regardless of the relaxation processes. If the value of γ' is known from experiment and n_g and p_g are not known, then one can use another form of this expression:

$$\tilde{\sigma}_g(\omega) = (\tilde{\sigma}_g)_{\max} \frac{\pi}{I_{\max}} \left(\frac{\omega_g}{\omega} \right)^2. \quad (26)$$

Here $(\tilde{\sigma}_g)_{\max}$ is the maximum value of the interband conductivity and I_{\max} is a quantity determined from Fig. 4.

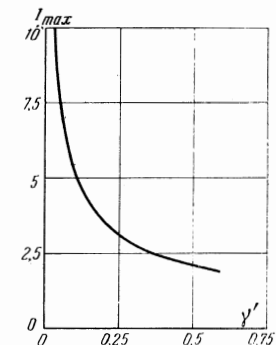


FIG. 4. Dependence of I_{\max} on the parameter γ' .

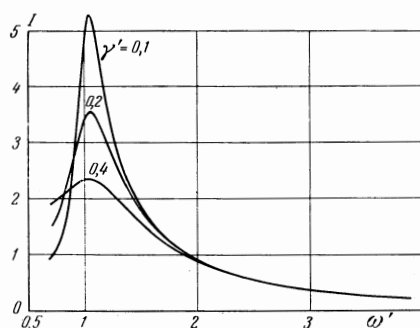


FIG. 5. Dependence of I on ω' for different values of the parameter γ' .

The parameter γ' which characterizes the relative diffuseness of the energy level, can be determined if the form of the dependence $I(\omega')$ is known. It is better to determine it by using the long-wave part of the curve $I(\omega')$. We consider a point on the curve $I(\omega')$ whose abscissa is equal to $\omega'_{\max} - \gamma'$. We denote the ordinate of this point by $I_{\gamma'}$. The results of calculation of $I_{\gamma'}$ for different values of the parameter γ' are given in Fig. 5, where the ratio $I_{\gamma'}/I_{\max}$ is plotted along the ordinate and γ' along the abscissa. It is seen from Fig. 6 that for $\gamma' < 0.4$ the ratio $I_{\gamma'}/I_{\max} \approx 0.7$. This means that in the zeroth approximation one can determine γ' from the experimental dependence of $\tilde{\sigma}(\omega)$, determining the abscissa of the point whose ordinate amounts to $\sim 70\%$ of the maximum ordinate, according to the relation $\gamma' = t(\omega_{\max} - \omega_{\gamma})/\omega_{\max}$. Here ω_{γ} is the abscissa of the point mentioned above. Further, this value of γ' can be made more precise by the method of successive approximations with the use of Fig. 6.

4. Let us compare our results with experiment. The structure of the interband transitions is most clearly marked, as our measurements have shown,^[4,8,10] at liquid helium temperatures. Therefore, for the corresponding comparison, it is desirable to use the results of the measurement of optical constants at low temperatures. Unfortunately, such measurements have been carried out only for a small number of metals. Below we give a comparison of the calculations with the experimental results for aluminum and indium.

Aluminum is a very favorable object for such a comparison, inasmuch as a strong band, associated with V_{200} , is situated in the region of 0.85μ , well isolated from other bands. Unfortunately, there are no low temperature measurements in this region. This band has been investigated in most detail at room tem-

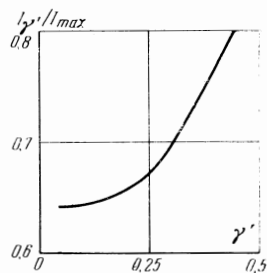


FIG. 6. Dependence of the value of $I_{\gamma'}/I_{\max}$ on γ' .

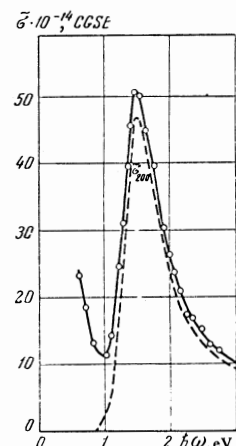


FIG. 7. Dependence of $\tilde{\sigma}_{200}$ on ω for aluminum. The solid curve for $\tilde{\sigma}$ is drawn through the experimental points; the dashed curve is $\tilde{\sigma}_{200}$ (room temperature).

perature by Shklyarevskii and Yarovaya,^[11] the results of whom are in good qualitative agreement with the results of Schultz and Tangherlini.^[12] In addition to these researches, one can also point out the work of Ehrenreich, Philipp and Segall,^[13] in which the band mentioned has also been investigated. However, the results of the latter research are represented in the form of a graph, from which it is not possible to determine either the parameters or the shape of the band of interest to us with any precision.

With the help of the data of^[11], we computed the total conductivity $\sigma = \tilde{\sigma} + \sigma_e$, where σ_e is the contribution to the conductivity from the free electrons. The quantity σ_e was determined from the results of our measurements of the optical constants of aluminum in the infrared region of the spectrum³⁾^[14] from the formulas of^[8]. In the region of the maximum of σ , the contribution of the electrons to the conductivity is small, less than 10%. The interband conductivity thus determined is equal to $\tilde{\sigma} = \tilde{\sigma}_{200} + \tilde{\sigma}_{111}$. The contribution of the band $\tilde{\sigma}_{111}$ in the spectral region of interest to us is less than 10%. It was determined by extrapolation according to the law $1/\omega^2$ of the curve $\tilde{\sigma}(\omega)$ in the region 0.62–0.83 eV (2.0 – 1.5 μ).

In Fig. 7 the dependence of $\tilde{\sigma}$ on ω for aluminum is shown by the continuous curve, and $\tilde{\sigma}_{200}(\omega)$ by the dashed curve. The maximum of this band is located at $\hbar\omega = 1.50 \pm 0.01$ eV. The determination of the quantity γ'_{200} , which is carried out by the method described above, gives $\gamma'_{200} = 0.09$. Here $t = 1.04$ and $V_{200} = 0.72$ eV. This is an excellent agreement with the value $V_{200} = 0.76$ eV obtained from the de Haas–van Alphen effect in^[2]. Comparison of Fig. 7 with Fig. 5 shows that the shapes of the theoretical and experimental curves are very similar.

In aluminum there is a second band associated with the potential V_{111} . The maximum of this band is located in the vicinity of 0.4 eV. Inasmuch as σ_e here is several times larger than $\tilde{\sigma}$ and, moreover, γ' for this band is relatively large, one can consider only the location of this maximum. Using the results obtained

³⁾The following parameters relating to electron conductivity were used: $N_{\text{opt}} = 7.02 \times 10^{22} \text{ cm}^{-3}$, $\nu = 1.2 \times 10^{14} \text{ sec}^{-1}$, $\beta_2 = 0.168$, $\beta_1/\lambda^2 = 3.3 \times 10^{-4} \mu^{-2}$. The calculation of σ_e was carried out according to Eqs. (9)-(10) of^[4].

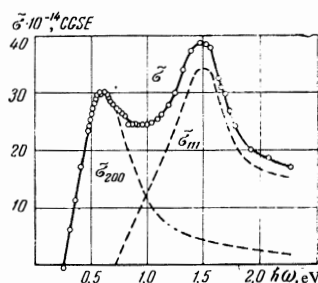


FIG. 8. Interband conductivity σ in indium, associated with Bragg reflections. The solid line passes through the experimental points, the dashed lines are the bands $\tilde{\sigma}_{111}$ and $\tilde{\sigma}_{200}$. $T = 4.2^\circ\text{K}$.

previously in^[14], and taking into account the contribution from σ_e and $\tilde{\sigma}_{200}$, we find that the maximum of $\tilde{\sigma}_{111}$ is located at $\hbar\omega = 0.44 \pm 0.06$ eV. Considering the error in the determination of ω_{max} , one can neglect the difference of t from unity. Then $V_{111} = 0.22 \pm 0.03$ eV. This also agrees excellently with the value obtained by Ascroft^[2] from the deHaas-van Alphen effect: $V_{111} = 0.24$ eV.

In indium, measurements at liquid helium temperatures show that there are two clearly marked bands in the region 0.6 and 1.5 eV. Their identification is not so unambiguous as in aluminum. Inasmuch as in indium there should be eight $\{111\}$ planes, four (200) and (020) planes and two (002) planes, we assume that the principal maximum in the region of 1.5 eV is associated with the $\{111\}$ planes, the second maximum with the $\{200\}$ planes. We did not find the third maximum up to 0.1 eV.

Figure 8 shows the experimental values of the interband conductivity $\hat{\sigma}$. Both bands intersect. Their distribution was completed in the following way. We assume that the contribution of $\tilde{\sigma}_{111}$ in the region of the maximum of $\tilde{\sigma}_{200}$ is negligibly small. This allows us to determine the value of γ'_{200} from the experimental curve. Furthermore, according to Eq. (26), the contribution of the band σ_{200} was calculated in the region $\hbar\omega > 1.2$ eV. This allows us to find the band $\tilde{\sigma}_{111}$. Then in the region $\hbar\omega < 1.2$ eV the values of $\tilde{\sigma}_{111}$ are found by linear extrapolation. This in turn made it possible to find the band $\tilde{\sigma}_{200}$ more precisely. In Fig. 8, the bands $\tilde{\sigma}_{111}$ and $\hat{\sigma}_{200}$ are shown by the dashed curves. After separation, we found $\gamma'_{111} = 0.16$ and $\gamma'_{200} = 0.25$.

The location of the maxima of these bands allows us to determine the values of the Fourier components of the pseudopotentials. For the band $\tilde{\sigma}_{111}$, the value of $\hbar\omega_{\text{max}} = 1.48 \pm 0.02$ eV, and according to Eq. (25), with the use of Fig. 3, we get $|V_{111}| = 0.70 \pm 0.01$ eV. For the band $\hat{\sigma}_{200}$, the value of $\hbar\omega_{\text{max}} = 0.60 \pm 0.02$ eV, and $|V_{200}| = 0.28 \pm 0.01$ eV. The determination of these quantities by the deHaas-van Alphen effect has evidently not been carried out. In the work of Mina and Khaikin,^[15] these quantities were found from cyclotron resonance. The authors obtained $|V_{111}| = 0.31 \pm 0.09$ eV, $|V_{200}| = 0.25 \pm 0.05$ eV. The values of V_{200} found from both experiments are identical. The divergence for V_{111} is significant. It greatly exceeds the errors of measurement. The reason for the divergence is not yet clear to us.

The found values of γ' allow us to estimate the absolute value of the maxima of $\tilde{\sigma}$ and compare them with the experimental values. For the $\{200\}$ band of aluminum, calculation gives $\tilde{\sigma}_{\text{max}} = 24 \times 10^{14}$ cgs units,

with the experimental value 46×10^{14} . For the $\{111\}$ band of indium, the calculated value is $\tilde{\sigma}_{\text{max}} = 17 \times 10^{14}$, the experimental, 34×10^{14} . For the second band of indium $\{200\}$, the calculated value⁴⁾ is $\tilde{\sigma}_{\text{max}} = 12 \times 10^{14}$. The disparity of the experimental and theoretical absolute values of $\tilde{\sigma}$ is by about a factor of two. This can be connected with the broadening of the experimental curves because of the simultaneous action of several planes, which was not taken into account by us. Account of this circumstance leads to a decrease in γ' and an increase in the computed values of $\tilde{\sigma}_{\text{max}}$.

The experiment shows that the diffusing of the levels of σ is large in all cases. Even at liquid helium temperatures, for indium, the collision frequencies ν_g , determined from γ' , are equal to $\nu_{111} = 7 \times 10^{14} \text{ sec}^{-1}$, $\nu_{200} = 4 \times 10^{14} \text{ sec}^{-1}$. This greatly exceeds the collision frequency of conduction electrons, which is equal to $0.6 \times 10^{14} \text{ sec}^{-1}$ for indium. This question should be discussed separately.

Thus, it can be assumed that the experiment confirms the theory. The structure of the absorption band in the visible and near infrared regions of the spectrum for polyvalent metals is determined on the basis of the interband transitions, which are connected with Bragg reflections. The optical properties permit us to determine the Fourier components of the pseudo-potential with great accuracy. The results of this research also show that for nontransition metals, the approximation of weak coupling serves also for the description of interband transitions in the visible and infrared portions of the spectrum.

In conclusion, we express our gratitude to L. V. Keldysh and R. N. Gurzhi for discussion of the results of the present research.

¹W. A. Harrison, Phys. Rev. 116, 555 (1959), 118, 1182, 1190 (1960).

²N. W. Ascroft, Phil. Mag. 8, 2055 (1963).

³J. R. Anderson and A. V. Gold, Phys. Rev. 139, A1459 (1965).

⁴A. I. Golovashkin, I. S. Levchenko, G. P. Motulevich and A. A. Shubin, Zh. Eksp. Teor. Fiz. 51, 1622 (1966) [Sov. Phys.-JETP 24, 1093 (1967)].

⁵L. Van Hove, Phys. Rev. 89, 1189 (1953); J. C. Phillips, Phys. Rev. 104, 1263 (1956).

⁶J. C. Phillips, Phys. Chem. Solids, 12, 208 (1960); D. Brust J. C. Phillips and F. Bassani, Phys. Rev. Lett. 9, 94 (1962).

⁷W. A. Harrison, Phys. Rev. 147, 467 (1966).

⁸A. I. Golovashkin and G. P. Motulevich, Zh. Eksp. Teor. Fiz. 53, 1526 (1967) Sov. Phys.-JETP 26, 881 (1968)].

⁹I. M. Ryzhik and I. S. Gradshteyn, Tables of Integrals, Sums, Series and Products, Academic Press, 1966.

⁴⁾In the calculation we assumed $n_{200} = 6$, which means $|V_{200}| \approx |V_{002}|$. This assumption is in agreement with the absence of the third band in the infrared region.

¹⁰A. I. Golovashkin and G. P. Motulevich, Zh. Eksp. Teor. Fiz. 47, 64 (1964) [Sov. Phys.-JETP 20, 44 (1965)].

¹¹I. N. Shklyarevskii and R. G. Yarovaya, Optika i spektroskopiya 16, 85 (1964).

¹²L. G. Schulz, JOSA 44, 357 (1954), L. G. Schulz and F. R. Tangherlini, JOSA 34, 362 (1954).

¹³H. Ehrenreich, H. R. Philipp and B. Segall, Phys. Rev. 132, 1918 (1963).

¹⁴A. I. Golovashkin, G. P. Motulevich and A. A. Shubin, Zh. Eksp. Teor. Fiz. 38, 51 (1960) [Sov. Phys.-JETP 11, 38 (1960)].

¹⁵R. T. Mina, M. S. Khaikin, Zh. Eksp. Teor. Fiz. 51, 62 (1966) [Sov. Phys.-JETP 24, 62 (1967)]. R. T. Mina, Paper presented at LT-10, Moscow, 1966, p. 254.

Translated by R. T. Beyer
233